Acta Cryst. (1987). B**43**, 319-325

Structure, Absolute Configuration and Optical Actvity of α-Nickel Sulfate Hexahydrate

By K. Stadnicka

Faculty of Chemistry, Jagiellonian University, ul. Karasia 3, 30-060 *Kraków, Poland*

A. M. Glazer

*Clarendon Laboratory, University of Oxford, Parks Road, Oxford OX*1 3*PU, UK*

and M. Koralewski

Institute of Physics, Adam Mickiewicz University, ul. Grunwaldzka 6, 60-780 *Poznań, Poland*

(*Received* 16 *September* 1986; *accepted* 19 *February* 1987)

Abstract

The crystal structure and the absolute configuration of α-$NiSO_4.6H_2O$ ($M_r = 262{\cdot}86$) have been determined by X-ray diffraction at room temperature. For a crystal that is optically laevo at 0·4579 μm, laevo at 0·4765 μm and dextro at 0·5145 μm, the space group was found to be $P4_12_12$ (D_4^4), with $a = 6{\cdot}783\,(1)$, $c = 18{\cdot}288\,(2)$ Å, $V = 841{\cdot}4\,(3)$ Å^3, $Z = 4$, $D_x = 2{\cdot}075$ Mg m^{-3}, Mo $K\alpha$, $\lambda = 0{\cdot}71069$ Å, $\mu = 2{\cdot}58$ mm^{-1}, $F(000) = 544$. The structure was refined to $R = 0{\cdot}0254$ and $R_G = 0{\cdot}0327$ for 1864 reflections. The chiral arrangement of O atoms in the structure is examined in connection with the theory of Glazer & Stadnicka [*J. Appl. Cryst.* (1986), **19**, 108-122] and linked with the measured optical rotation at wavelengths below ~0·5 μm and above ~2·0 μm. It is shown that the contribution from the O atoms of the water of crystallization is more important than that from the sulfate O atoms in determining this part of the optical rotatory dispersion, whereas the observed anomalies between these wavelengths are principally due to d-d transitions in the nickel ion. Calculations using the program of Devarajan & Glazer [*Acta Cryst.* (1986), A**42**, 560-569] support this view.

Introduction

Ever since the discovery of optical activity by Arago in 1811, there have been many attempts at explaining its origin. In order to understand optical activity in crystals it is important first to determine both the chirality (or absolute structure) of the crystal and its optical rotation - the so-called *absolute configuration.* Although it has been possible for the last 40 years or so to use X-ray anomalous scattering to determine absolute configuration, there are relatively few examples to be found in the literature. Those inorganic crystals for which the true absolute configuration is known were shown by Glazer & Stadnicka (1986) to have structural helices of polarizable atoms, whose sense could be related closely to the sense of rotation of plane-polarized light. A set of rules was given to enable these helices to be correctly chosen. Devarajan & Glazer (1986) subsequently used a polarizable point dipole approach based on the original work of Born and others to calculate optical rotations for most of the inorganic crystals studied by Glazer & Stadnicka.

The first structure determination of α-$NiSO_4.6H_2O$ was carried out by Beevers & Lipson (1932), who obtained the space group $P4_12_12$ (or $P4_32_12$) and so predicted the occurrence of right and left crystals which should possess rotatory powers of opposite sign. They confirmed their predictions and discovered anomalous behaviour of the rotatory power. After this work, many papers were published on the optical properties, which have been shown to be anomalous for this material. Below, we briefly survey some of the more important papers.

The optical rotatory dispersion (ORD) was measured for the first time quantitatively by Underwood, Slack & Nelson (1938), who showed that between 0·420 and 0·650 μm the sign of rotation changed at 0·503 μm. Absorption bands at 0·3890 and 0·7187 μm were also observed. Slack, Lageman & Underwood (1938) also measured the magneto-optical activity, and calculated an effective optically active ultraviolet absorption band at 0·0964 μm.

A nearly complete measurement of ORD, circular dichroism (CD) and absorption was published by Ingersoll, Rudnick, Slack & Underwood (1940) over the wavelength range 0·25-2·2 μm. Striking anomalies in the ORD were found at 0·69 and 1·16 μm, corresponding to absorption and CD maxima at these wavelengths. Of the observed bands shown to contribute to the ORD, those at 0·385 and 0·690 μm were identified as being responsible for the green colour characteristic of divalent nickel hydrates, with one at 1·16 μm probably belonging to the same system of bands. Two absorption bands at about 1·5 and 2·0 μm were identified as being due to

0108-7681/87/040319-07$01.50

the water of crystallization, and, because of their vibrational character, considered to make no appreciable contribution to the ORD. A theoretical relation between rotatory power and CD was also verified.

In 1966, O'Connor & Dale published a two-dimensional neutron diffraction study of the crystal structure of the deuterated compound. They confirmed the space-group assignment and basic structure determination of Beevers & Lipson and, in addition, found all the deuterium positions.

Further work on the CD and absorption spectra was published by Grinter, Harding & Mason (1970). In this paper, which gives several other references to studies of the ORD and electronic bands of $NiSO_4.6H_2O$, all the bands were assigned group theoretical symbols relating to *d-d* transitions within the electronic states of the quasi-octahedral $[Ni(OH_2)_6]^{2+}$ moiety. Their results indicated that neither first-order spin-orbit coupling nor trigonal, tetragonal or orthorhombic distortions significantly affect the accessible electronic states involved in the transitions.

The only theoretical analyses of the optical activity in this crystal appear to have been made by Strickland & Richardson (1972) and Kato (1972), who demonstrated that the CD bands in the near infra-red, visible and near ultraviolet regions could be successfully calculated on the basis of a model in which the $Ni(OH_2)_6$ groups were considered to be isolated from one another, but perturbed by the field due to the crystal environment with site symmetry $2(C_2)$. Thus the optical activity related to these bands was found not to be attributed to the interaction between chromophores constituting a structural helix, but to the asymmetric field on the metal ions.

Burkov, Kizel, Ivanova, Safronov, Semin & Chel'tsov (1973) measured the ORD for the sulfate and selenate crystals, and showed that it was similar in both. Castaño (1969) and Perekalina, Kaldybaev & Konstantinova (1979) measured the CD tensor components (parallel and perpendicular to the tetragonal *c* axis) and their dispersion within the wavelength range 0·35–0·50 μm. These turned out to be opposite in sign, but their magnitudes varied with wavelength in a similar fashion, peaking at about 0·390 μm.

Despite the many papers dealing with the subject of optical activity in α-$NiSO_4.6H_2O$, there has not been any measurement made of the absolute configuration of this crystal nor any attempt, therefore, to link its chirality with that of the optical rotation. The most recent structure determination that we have found is by Bargouth & Will (1981), but although the structure was refined to an *R* factor of about 2%, no absolute configuration was reported. In the present paper, we describe a new X-ray structure determination, including for the first time the absolute configuration. We also discuss the optical rotatory dispersion in connection with the work of Glazer & Stadnicka (1986) and of Devarajan & Glazer (1986). It is important to realise that all other studies of optical activity in this compound have so far concentrated exclusively on the *d-d* transitions in the metal ion, and therefore relate only to the relevant CD and absorption bands within the observable wavelength range. We, on the other hand, concentrate on the underlying behaviour of the ORD, which is best seen at wavelengths outside the region influenced by these *d-d* transitions. It will be shown that this arises mainly from the crystal structural arrangement of the O atoms of the water molecules.

Crystal preparation and optical measurements

Analytically pure $NiSO_4.7H_2O$ (from Polskie Odczynniki Chemcizne) was recrystallized three times from water, and then made into a saturated aqueous solution. Single crystals of α-$NiSO_4.6H_2O$ were grown by slow evaporation of the solution at about 308 K. Large dark-green, bypyramidal crystals were obtained, typically about 40 mm long and 25 mm across, and of good optical quality.

A 4·8 mm thick (001) slice was cut for measurements of the ORD at room temperature. The orientation was checked by conoscopic figures, and the optical rotatory power was measured by the modulation method described by Habryło & Koralewski (1981). An argon-ion laser (Zeiss Jena) was used as the light source, and this enabled measurements to be made at three wavelengths, 0·4579, 0·4765 and 0·5145 μm. The sign of the optical rotation was checked by rotation of an analyser and also by inspection of Airy's spiral.

Absorption measurements were also made at room temperature in the UV and visible regions (0·185–0·9 μm) on a 1·18 mm (001) slice, using a Specord M40 (Zeiss Jena) spectrometer with unpolarized light.

Structure determination

A small piece of the crystal of α-$NiSO_4.6H_2O$ used in the ORD measurements was cut in the shape of a parallelepiped with {001} and {110} faces, and measuring 0·28 (2) mm between (0,0,1) and $(0,0,\bar{1})$, 0·32 (2) mm between $(\bar{1},1,0)$ and $(1,\bar{1},0)$, and 0·42 (2) mm between (1,1,0) and $(\bar{1},\bar{1},0)$. X-ray measurements were made at room temperature on an Enraf-Nonius CAD-4 diffractometer using graphite-monochromated Mo $K\alpha$ radiation ($\lambda = 0·71069$ Å). The lattice parameters $a = 6·783$ (1), $c = 18·288$ (2) Å were obtained by a least-squares fit using 25 reflections in the range $11 \leq \theta \leq 19°$. The intensity data were collected up to $\theta = 36°$ in the θ–2θ scan mode, with the scan width given by $(0·75 + 0·35 \tan \theta)°$. Two intensity control reflections were monitored hourly throughout the data collection and showed no systematic changes: the average variation was less than

Table 1. *Fractional coordinates and thermal parameters with e.s.d.'s in parentheses*

$T=\exp[-2\pi^2(U_{11}h^2a^{*2}+\cdots+2U_{12}hka^*b^*+\cdots)]$, where U_{ij} are in Å^2. For H atoms, the isotropic value of U is given.

	Site	Point symmetry	x	y	z
Ni	4(a)	..2	0·21060 (3)	0·216060 (3)	0·00000
S	4(a)	..2	0·70943 (6)	0·70943 (6)	0·00000
O(1)	8(b)	1	0·1727 (2)	−0·0470 (2)	0·0528 (1)
O(2)	8(b)	1	0·4705 (2)	0·2449 (2)	0·0561 (1)
O(3)	8(b)	1	0·0658 (2)	0·3599 (2)	0·0850 (1)
O(4)	8(b)	1	0·6209 (2)	0·6203 (2)	0·0658 (1)
O(5)	8(b)	1	0·9237 (2)	0·6731 (2)	0·0003 (1)
H(11)	8(b)	1	0·1097 (6)	−0·1333 (6)	0·0394 (6)
H(12)	8(b)	1	0·2215 (6)	−0·0746 (6)	0·0867 (5)
H(21)	8(b)	1	0·5702 (6)	0·1559 (6)	0·0507 (6)
H(22)	8(b)	1	0·5371 (6)	0·3532 (6)	0·0601 (6)
H(31)	8(b)	1	−0·0051 (6)	0·4453 (6)	0·0744 (6)
H(32)	8(b)	1	−0·0101 (6)	0·2941 (6)	0·1149 (5)

	U_{11}	U_{22}	U_{33}	U_{23}	U_{13}	U_{12}
Ni	0·0142 (1)	0·0142 (1)	0·0135 (1)	0·0005 (1)	−0·0005 (1)	−0·0015 (1)
S	0·0147 (1)	0·0147 (1)	0·0203 (2)	−0·0014 (1)	0·0014 (1)	−0·0006 (2)
O(1)	0·0335 (5)	0·0245 (4)	0·0284 (4)	0·0123 (4)	−0·0125 (4)	−0·0128 (4)
O(2)	0·0165 (4)	0·0193 (4)	0·0287 (4)	−0·0032 (4)	−0·0040 (4)	−0·0005 (4)
O(3)	0·0219 (4)	0·0212 (4)	0·0188 (4)	0·0001 (4)	0·0013 (4)	0·0042 (4)
O(4)	0·0478 (5)	0·0221 (4)	0·0242 (4)	0·0002 (4)	0·0108 (4)	−0·0091 (4)
O(5)	0·0170 (4)	0·0248 (4)	0·0418 (4)	−0·0074 (4)	−0·0045 (4)	0·0058 (4)
H(11)	0·0487 (6)					
H(12)	0·0506 (6)					
H(21)	0·0504 (6)					
H(22)	0·0491 (6)					
H(31)	0·0516 (6)					
H(32)	0·0502 (6)					

Table 2. *Important interatomic distances and angles*

(a) Bond lengths (Å) and angles (°)

Ni–O(1)	2·013 (1)	O(1)–H(12)	0·728 (9)
Ni–O(2)	2·053 (1)	O(2)–H(21)	0·912 (4)
Ni–O(3)	2·086 (2)	O(2)–H(22)	0·865 (4)
S–O(4)	1·475 (2)	O(3)–H(31)	0·798 (5)
S–O(5)	1·474 (1)	O(3)–H(32)	0·860 (7)
O(1)–H(11)	0·765 (5)		

O(1)–Ni–O(2)	88·2 (1)	O(3)–Ni–O(3^{i})	179·9 (1)
O(1)–Ni–O(3)	89·6 (1)	O(4)–S–O(5)	109·2 (1)
O(1)–Ni–O(1^{i})	90·5 (1)	O(4)–S–O(4^{i})	109·4 (1)
O(1)–Ni–O(3^{i})	90·5 (1)	O(4)–S–O(5^{i})	109·9 (1)
O(2)–Ni–O(3)	88·8 (1)	O(5)–S–O(5^{i})	109·3 (1)
O(2)–Ni–O(2^{i})	93·2 (1)	H(11)–O(1)–H(12)	109·3 (7)
O(2)–Ni–O(3^{i})	91·1 (1)	H(21)–O(2)–H(22)	100·6 (4)
O(1)–Ni–O(2^{i})	180·0 (1)	H(31)–O(3)–H(32)	99·5 (6)

(b) Geometry of hydrogen bonding

D–H$\cdots A$	H$\cdots A$ (Å)	$D\cdots A$ (Å)	∠ DHA (°)
O(1)–H(11)$\cdots$O(5^{ii})	1·956 (5)	2·716 (2)	172·3 (6)
O(1)–H(12)$\cdots$O(3^{v})	2·087 (6)	2·792 (2)	163·2 (5)
O(2)–H(21)$\cdots$O(5^{iii})	1·959 (5)	2·775 (2)	166·4 (5)
O(2)–H(22)$\cdots$O(4)	1·902 (4)	2·749 (2)	165·8 (4)
O(3)–H(31)$\cdots$O(5^{iv})	2·110 (7)	2·820 (2)	148·2 (8)
O(3)–H(32)$\cdots$O(4^{vi})	1·887 (4)	2·729 (2)	165·8 (4)

(c) Non-bonding distances (Å) less than 3·100 Å

O(1)–O(2)	2·829 (2)	O(2)–O(2^{i})	2·982 (2)
O(1)–O(3)	2·888 (2)	O(3)–O(2^{i})	2·956 (2)
O(2)–O(3)	2·895 (2)	O(4)–O(4^{i})	2·408 (2)
O(4)–O(5)	2·405 (2)	O(5)–O(4^{i})	2·414 (2)
O(1)–O(1^{i})	2·858 (2)	O(5)–O(5^{i})	2·404 (2)
O(3)–O(1^{i})	2·911 (2)	O(2)–O(1^{vi})	3·097 (2)

Symmetry code: (i) $y, x, -z$; (ii) $-1+x, -1+y, z$; (iii) $y, -1+x, -z$; (iv) $-1+x, y, z$; (v) $\frac{1}{2}-x, -\frac{1}{2}+y, \frac{1}{4}-z$; (vi) $\frac{1}{2}-x, \frac{1}{2}+y, \frac{1}{4}-z$.

1·4%. 4009 reflections with $I>\sigma(I)$ were measured in the range $0\le h\le 11$, $0\le k\le 11$, $-30\le l\le 30$. These were corrected for Lp factors and absorption using the *SHELX*76 program (Sheldrick, 1976); the maximum and minimum transmission factors were 0·531 and 0·456 respectively. Symmetrically equivalent reflections were then averaged ($R_{\rm int}=$ 0·027) to give 1886 unique mean values of $|F(hkl)|$. Refinement of 1864 values of $|F(hkl)|>2\sigma$ was carried out with the *SHELX*76 program in both enantiomorphic space groups incorporating neutral atomic scattering factors and anomalous-scattering factors from *International Tables for X-ray Crystallography* (1974). The initial coordinates for non-H atoms were taken from O'Connor & Dale (1966). In the course of the refinement, the H atoms were located on Fourier difference maps. The temperature factors for all atoms except H were refined anisotropically. In the final stages of the refinement, no peaks were found on Fourier difference maps above 0·2 e Å^{-3}, thus showing that all atoms had been accounted for. For space group $P4_12_12$ the final agreement factors were $R=0{\cdot}0254$, $R_G=0{\cdot}0327$; $\Delta/\sigma=0{\cdot}05$ for non-H atoms, 0·25 for H atoms. Refinement in space group $P4_32_12$ with the coordinates inverted (equivalent to changing the sign of f'') gave $R=0{\cdot}0446$, $R_G=$ 0·0589. Recalculation of structure factors for the models $P4_12_12$ ($\bar{x}\bar{y}\bar{z}$) and $P4_32_12$ (xyz) [in the same way as done by Glazer, Stadnicka & Singh (1981) for dicalcium strontium propionate, which crystallizes in the same space group] gave $R\sim 0{\cdot}16$ and $R_G\sim 0{\cdot}53$. There was therefore no doubt that the crystal belonged to the $P4_12_12$ (xyz) enantiomorph. The final atomic coordinates and temperature factors are given in Table 1 and important interatomic distances and angles in Table 2.[*]

Atoms O(1), O(2) and O(3) belong to the water molecules and form a roughly octahedral coordination polyhedron (Fig. 1) around the Ni^{2+} ion, which occurs on a 4(a) site with symmetry 2(C_2). O(2) and O(3) are each connected through two hydrogen bonds (Table 2b) to the sulfate O(4) and O(5) atoms, which act as acceptors. For O(1) the acceptors are O(5) and the water O(3) on a neighbouring coordination polyhedron (Fig. 2a).

The average O–O distance within the polyhedron is 2·903 (2) Å. This should be compared with the average hydrogen-bonded distance of 2·760 (2) Å. O(4) and O(5) in the sulfate group (Figs. 1 and 2b), have an average separation of 2·408 (2) Å, emphasizing the great difference between the water O atoms on the one hand and the sulfate O atoms on the other. This too can be seen by comparing the Ni–O and S–O distances, in which the latter are considerably shorter. Of the remaining interatomic distances between the polyhedra, only one is close to 3·1 Å (Table 2c), and all others are much longer.

---

[*] A list of structure factors has been deposited with the British Library Document Supply Centre as Supplementary Publication No. SUP 43764 (9 pp.). Copies may be obtained through The Executive Secretary, International Union of Crystallography, 5 Abbey Square, Chester CH1 2HU, England.

It can be seen (Fig. 2*b*) that the structure is comprised of layers of SO_4 and $Ni(OH_2)_6$ groups connected not only by a network of hydrogen bonds *within* a layer, but also by hydrogen bonds *between* the layers. The layers are stacked in such a way that the $Ni(OH_2)_6$ coordination polyhedra are grouped around the 4_1 axes, with the sulfate groups almost directly above along [001] and alternating with them every half *c* repeat. The effect of this stacking arrangement is to produce channels along the 4_1 axes in which only H atoms occur. O(1) and O(3) form a 'helical' structure (Fig. 3), which in projection has reentrant angles caused by the strong hydrogen bonds to O(4) and O(5). Although O(2) lies in the vicinity, it cannot be considered to be part of the helix.

We must also comment on some of the drawings of this structure appearing in the literature, which are either wrong or misleading. Thus, for example, in Strickland & Richardson (1972) and in Kato, Ban & Tsujikawa (1972) the number of sulfate groups around the $Ni(OH_2)_6$ polyhedron is shown to be less than six. This probably arises from earlier statements that there are stong hydrogen bonds within (001) layers with weak hydrogen bonds between the layers; our measurements show that the hydrogen bonds between the layers are just as strong as the others. We have a more serious objection to the drawing in Kato *et al.* (their Fig. 2) which shows four $Ni(OH_2)_6$ polyhedra in the unit cell positioned in such a way that they appear to be approximately related by a fourfold axis projected in the centre of the unit cell, whereas our Fig. 2(*a*) clearly shows this to be far from the truth. Unfortunately, their inaccurate

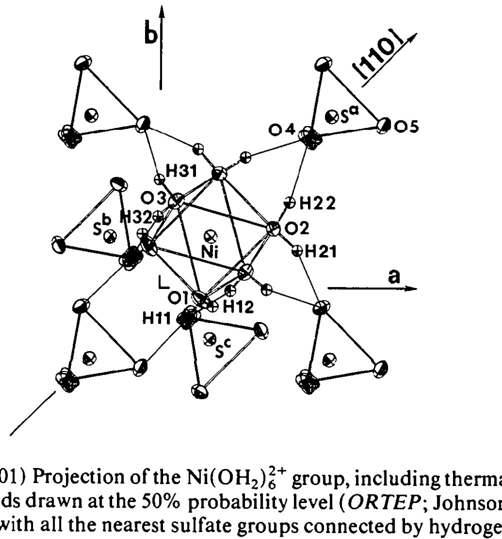

Fig. 1. (001) Projection of the $Ni(OH_2)_6^{2+}$ group, including thermal ellipsoids drawn at the 50% probability level (*ORTEP*; Johnson, 1965), with all the nearest sulfate groups connected by hydrogen bonds (marked by thin lines). O–O contacts are denoted by double lines. H(11) is not easily seen as it projects directly onto two O(4) ellipsoids. The fractional heights along *c* for the atoms labelled in the figure are: Ni, 0·00; S^a, 0·00; S^b, 0·25; S^c, −0·25; O(1), 0·0528; O(2), 0·0561; O(3), 0·0850; O(4), 0·0658; O(5), 0·0003.

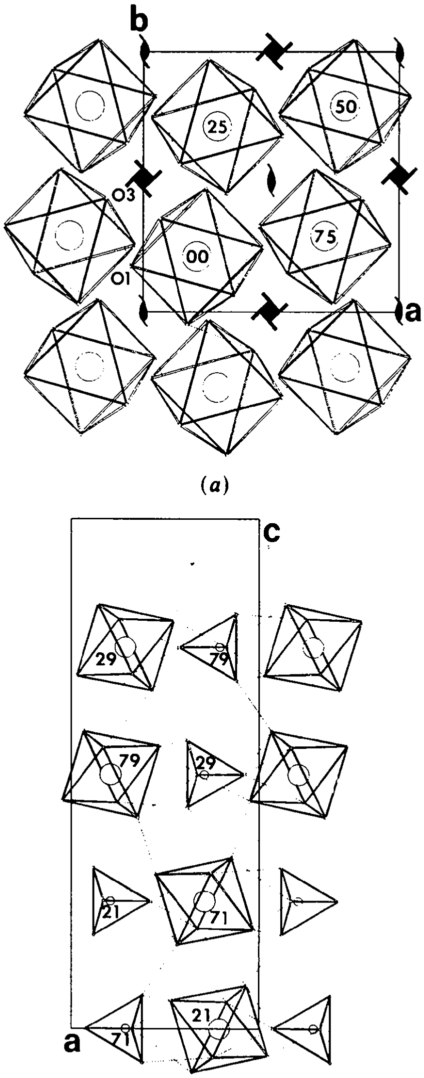

(*a*)

(*b*)

Fig. 2. (*a*) (001) Projection of NiO_6 coordination polyhedra (slightly distorted octahedra) showing how they are packed together. Hydrogen bonds between O(1) and O(3) of neighbouring polyhedra are shown dotted. Heights of Ni (large circles) are marked in 1/100's of *c*. 4_1 and 2_1 axes are marked. (*b*) (010) Projection of NiO_6 and SO_4 polyhedra with hydrogen bonds between O atoms shown dotted. The sulfate polyhedra are perfect tetrahedra within the limit of error. Heights of Ni (large circles) and of S (small circles) are marked in 1/100's of *b*.

Fig. 3. Stereo projection of the region around the 4_1 axis through $(0, \frac{1}{2}, z)$. O(1) and O(3) are seen to lie on an *RS*2/8 helix consisting of alternating O(3)–O(1) contacts (2·911 Å) and O(1)···O(3) hydrogen bonds (2·792 Å).

diagram has spread to other papers, *e.g.* Kizel, Krasilov & Burkov (1974).

Discussion

Fig. 4 shows plots of the ORD, CD and ordinary absorption spectra measured along [001], taken from several sources in order to provide a complete picture so far as is known. The short dotted line refers to ORD measurements carried out on our crystal over a limited wavelength range, and it is clear that our crystal has optical activity opposite to that shown in the experimental ORD curve marked by the dash-dot line in Fig. 4.

It can also be seen from this curve that the behaviour is anomalous in the way that the sign of rotation changes with wavelength at approximately 0·5 and 1·2 μm. There are in addition other anomalies at about 0·39 and 0·69 μm. The three major CD peaks have been identified by Grinter *et al.* (1970) as *d–d* transitions of the Ni^{2+} ion. Assuming the crystal field to be octahedral, these transitions were labelled as:

$$^3A_{2g}\to{}^3T_{1g}(P)$$

$$^3A_{2g}\to{}^1E_g,{}^3T_{1g}(F)$$

$$^3A_{2g}\to{}^3T_{2g}(F).$$

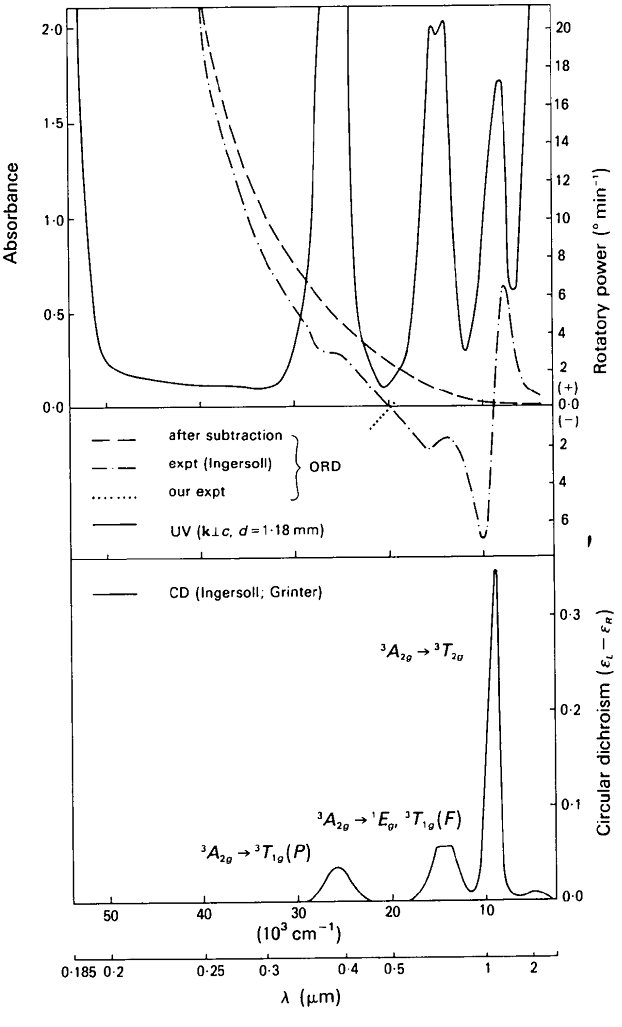

Fig. 4. ORD, CD and absorption spectra of α-$NiSO_4.6H_2O$. The measured ORD is marked in dash-dot lines, and the ORD calculated after removal of the contribution from the Ni^{2+} transitions is given by the curve marked in dashes. The small line of dots around 0·5 μm are our own measurements showing that the crystal used here was of opposite sign.

Table 3. *Spectral values used in the Kramers–Kronig formula given by equation* (1), *after Moscowitz* (1960)

	$^3A_{2g}\to{}^3T_{2g}$	$^3A_{2g}\to{}^1E_g,{}^3T_{1g}$	$3A_{2g}\to{}^3T_{1g}$
R_k (10^{-40} cgs)	1·7	0·25	0·07
Δ_k^0 (μm)	0·145	0·080	0·035
λ_k^0 (μm)	1·155	0·690	0·390

[Note that, strictly speaking, as the crystal field at the nickel site is $2(C_2)$, the group theoretical labels should be converted as:

$$A_{2g}\to A \qquad T_{1g}\to A+2B$$

$$E_g\to 2A \qquad T_{2g}\to A+2B$$

and so the observed peaks should be, at least in principle, split further.] In Table 3 the rotatory strengths R_k, calculated from the CD bands and the wavelength values of the CD maxima, λ_k^0, are given for these three transitions, as taken from Grinter *et al.* (1970). Assuming the peaks to be Gaussian, we also give the CD halfwidths Δ_k^0 measured from Fig. 4. The $^3A_{2g}\to{}^1E_g$, $^3T_{1g}$ peak actually has some fine structure (Meredith & Palmer, 1969), but at room temperature this is small, and for our purposes the assumption of a Gaussian shape is reasonable.

In order to calculate the contribution of the nickel *d–d* transitions to the observed ORD, we applied to each peak the Kramers–Kronig transformation given by Moscowitz (1960):

$$\rho_k=\frac{2R_k}{\pi(0{\cdot}696\times10^{-42})}\frac{\lambda_k^0}{\Delta_k^0}$$

$$\times\left\{\exp\left[-(\lambda-\lambda_k^0)^2/(\Delta_k^0)^2\right]\int_0^{(\lambda-\lambda_k^0)/\Delta_k^0}\exp(u^2)\,\mathrm{d}u\right.$$

$$\left.-\Delta_k^0/2(\lambda+\lambda_k^0)\right\} \qquad (1)$$

The resulting contributions between 0·25 and 0·65 μm were summed together, and then subtracted from the observed ORD curve within this spectral region. The resulting curve, which essentially reflects the contribution to the ORD from the O atoms alone, was fitted to the Drude-type analytical expression:

$$\rho=\frac{0{\cdot}6053}{\lambda^2-\lambda_0^2}-0{\cdot}3947 \qquad (2)$$

where λ is in μm, ρ is in ° mm^{-1} and $\lambda_0 = 0{\cdot}1876$ μm. This equation gives the dashed curve shown in Fig. 4. Comparing this theoretically derived curve with the experimental ORD curve, we now see that the O contribution provides the major underlying behaviour and the nickel contribution interposes to cause the relatively small anomalies and apparent complexity of the ORD curve within a limited wavelength range. It is probable that the large rise in absorption below 0·2 μm (*cf.* λ_0) in Fig. 4 is due to the O atoms and that it is the optically active band associated with the oxygen ORD curve that we have derived. Unfortunately, there have been no CD measurements published for this wavelength region (presumably because it is so difficult to do the experiment in the UV end of the spectrum), which would corroborate this assumption.

We note that in the isomorphous compound $ZnSeO_4.6H_2O$, the observed ORD curve is almost identical to our derived curve for oxygen, and that the absorption spectrum shows only a steep rise below about 0·23 μm (Kato *et al.*, 1972), which can be compared with the absorption edge observed in α-$NiSO_4.6H_2O$ at about 0·2 μm in Fig. 4. $NiSeO_4.6H_2O$, on the other hand, shows ORD, CD and absorption spectra that are almost identical to those of α-$NiSO_4.6H_2O$. Both observations support our view that the O atoms provide the general shape of the ORD curve and that the transition metal simply adds an extra contribution to modify this curve, thus causing the changes in sign.

Because the optical rotation in our crystal (laevo at 0·4579 and 0·4765 μm, dextro at 0·5145 μm) was found to be opposite in sign to the ORD curve in Fig. 4, as indicated by the dotted line, we would expect that the crystal would be overall laevo, *i.e.* negative, with respect to the oxygen curve that we have derived. It is important to compare this finding with what is known about the crystal structure.

Following Glazer & Stadnicka (1986) we first choose the most polarizable atoms, which, in this structure, are the O atoms. Because the Ni–O bonds are weaker than the S–O bonds (as shown by the relative bond distances), O(1), O(2) and O(3) will have larger electronic polarizabilities than O(4) and O(5), and so they should contribute more strongly towards the optical activity. In this complicated crystal structure, it is difficult to envisage the anisotropic polarizability ellipsoids, as done for the crystals studied by Glazer & Stadnicka, but it is interesting to note that the helix of O(1) and O(3) atoms in Fig. 3 is right-handed, *RS*2/8 in the notation of Glazer & Stadnicka, and so has the same hand as the sense of rotation of the plane-polarized light.

Table 4. *Examples of calculations of refractive indices and optical rotatory power along* [001] *at* $\lambda = 0{\cdot}50$ μm *from oxygen in* $NiSO_4.6H_2O$

Calculations according to the program of Devarajan & Glazer (1986). The results should be compared with the values estimated from experiment: $n_o = 1{\cdot}517$, $n_e = 1{\cdot}493$ and $\rho = -2{\cdot}4°\,\mathrm{mm}^{-1}$.

Polarizability volumes (Å^3)							
O(1)	O(2)	O(3)	O(4)	O(5)	n_o	n_e	ρ(° mm^{-1})
1·01	1·02	1·01	1·60	1·60	1·428	1·416	+0·86
1·80	1·40	1·80	1·40	1·40	1·544	1·544	+0·47
1·40	1·40	1·40	1·40	1·40	1·482	1·471	+0·29
1·20	1·00	1·20	1·00	1·00	1·353	1·351	+0·29
1·40	1·00	1·40	1·00	1·00	1·382	1·384	+0·26
2·20	1·50	2·20	1·50	1·50	1·640	1·653	−0·22
1·80	1·00	1·80	1·00	1·00	1·441	1·455	−0·29
1·40	1·90	1·40	1·00	1·00	1·453	1·448	−0·62
1·45	1·80	1·45	1·30	1·30	1·506	1·492	−1·15
1·50	1·80	1·50	1·30	1·30	1·514	1·501	−1·22
1·50	1·80	1·50	1·40	1·40	1·532	1·517	−1·23
1·60	1·90	1·60	1·00	1·00	1·483	1·484	−1·35
1·60	1·80	1·60	1·30	1·30	1·529	1·519	−1·43
1·70	2·00	1·70	1·00	1·00	1·507	1·510	−1·72
1·80	1·40	1·80	1·00	1·00	1·473	1·484	−1·84
1·70	2·00	1·70	1·20	1·20	1·544	1·540	−2·06
1·70	2·00	1·80	1·20	1·20	1·551	1·549	−2·27
1·80	2·00	1·70	1·20	1·20	1·552	1·548	−2·33
2·50	1·20	2·50	1·20	1·20	1·607	1·654	−2·35
1·80	1·90	1·80	1·00	1·00	1·514	1·522	−2·44
1·80	1·80	1·80	1·00	1·00	1·506	1·514	−2·46

We calculated the optical rotatory power due to the O atoms using the program described by Devarajan & Glazer (1986). This required estimated isotropic polarizabilities for each atom, atomic fractional coordinates, cell dimensions, wavelength of light and propagation direction to be supplied, and the program then calculated refractive indices and optical rotatory power *via* an Ewald sum over all the point dipoles in the crystal. We then varied the polarizabilities, keeping the closest possible agreement with the refractive indices, and examined the calculated value of ρ. In this crystal, there are five independent isotropic oxygen polarizabilities to adjust and so we could not expect to calculate the correct values as directly as in the crystals studied by Devarajan & Glazer. For an assumed wavelength of 0·50 μm, the estimated experimental value of ρ for the oxygen curve was obtained from equation (2) as $-2{\cdot}4°\,\mathrm{mm}^{-1}$, with the sign chosen as negative on the basis of our experimentally determined ORD. The refractive indices are only known for three wavelengths: 0·6563, 0·5893 and 0·4861 μm (Winchell & Winchell, 1964). To find the values at $\lambda = 0{\cdot}50$ μm we used the Sellmeier approximation to fit a smooth curve through the three wavelengths

$$n_o^2 = \frac{1{\cdot}23925\lambda^2}{\lambda^2 - 0{\cdot}012033} \qquad (3a)$$

$$n_o^2 = \frac{1{\cdot}173017\lambda^2}{\lambda^2 - 0{\cdot}011091} \qquad (3b)$$

where λ is in μm, and this gave $n_o = 1{\cdot}517$ nd $n_e = 1{\cdot}493$ (to use only three points in this way is dubious, of course, but in any case the refractive indices in this wavelength region show only a small dispersion).

Table 4 gives the results of several calculations where the five polarizabilities have been varied within acceptable limits for oxygen. To some extent, we find a conflict between the roles played by the water O(1), O(2) and O(3) atoms, on the one hand, and by the sulfate O(4) and O(5) atoms, on the other. Increasing the polarizabilities of O(1) and O(3) tends to give the correct sign of rotation but makes $n_o < n_e$, whereas increasing the polarizabilities of the sulfate O atoms tends to give the wrong sign of ρ but makes $n_o > n_e$. In addition, a small value for the O(2) polarizability tends to make $n_o < n_e$. Since the observed refractive indices must contain contributions from *all* the atoms, whereas our calculation is based purely on the O atoms, it may be that we should not put too much emphasis on trying to obtain $n_o > n_e$ in our computations. At the chosen wavelength, the optical rotatory power is small, and so the classical theory used cannot be expected to give a precise result. Furthermore, the oxygen curve obtained in Fig. 4 is based on the precision with which the Kramers-Kronig relationship can be applied and so it too probably has a substantial error in magnitude, although not in sign. It would be better to calculate ρ at shorter wavelengths, where the observed and estimated ORD curves are closer and the values of ρ are larger; but, unfortunately, we have not found any measurements of the refractive indices at these wavelengths, and it would be inadvisable to extrapolate the Sellmeier equation so far, especially because of the intervening electronic bands.

Despite the complexity of this case, our calculations do reveal clearly that it is the water O atoms that are more important than the sulfate O atoms in determining the sign and magnitude of the ORD at wavelengths below about 0·5 μm and above about 2·0 μm, where there is little influence from the nickel *d*-*d* transitions. It is also comforting to note that, at least as far as O(1) and O(3) are concerned, this result agrees with the Glazer & Stadnicka approach. However, the computation also requires a large polarizability from O(2), which does not form part of the *RS*2/8 structural helix, although it appears within its confines.

Finally, as further evidence of the correctness of the computations, it is worth pointing out that when we calculate ρ for a direction perpendicular to [001], we find that the sign is changed. This should be checked experimentally in the future, but for the present we note that it is consistent with the findings of Castaño (1969) and Perekalina *et al.* (1979).

Conclusions

The ORD of α-NiSO$_4$.6H$_2$O is anomalous in the visible region, but, nevertheless, we have demonstrated a link between the structural chirality, particularly arising from the water O atoms, and that of the rotation of plane-polarized light in the normal regions of the ORD curve, which have previously been ignored by other authors. A number of approximations have had to be made in this example, but, even so, the results of our computations are most encouraging. As with the examples used by Glazer & Stadnicka (1986) and by Devarajan & Glazer (1986), it is seen that the major influence on the optical properties comes from the structural arrangement of the atoms in the crystal.

KS is grateful to the British Council for funds which enabled the X-ray measurements to be made and to SLAFiBS (Kraków) for the use of the diffractometer. AMG wishes to thank the Jagiellonian University for supporting this collaborative research, and MK acknowledges the support of the British Council and Jesus College, Oxford for funding a visit to the Clarendon Laboratory. This work was partially supported by the Polish Academy of Sciences under the project CPBP 01.12.

References

Arago, F. (1811). *Mem. Cl. Sci. Math. Phys. Inst.* **12**, 93-134.
Bargouth, M. O. & Will, G. (1981). ICTP Report. International Centre for Theoretical Physics, Trieste.
Beevers, C. A. & Lipson, H. (1932). *Z. Kristallogr.* **83**, 123-135.
Burkov, V. I., Kizel, V. A., Ivanova, I. N., Safronov, G. M., Semin, G. S. & Chel'tsov, P. A. (1973). *Opt. Spektrosk.* **35**, 884-887 (in Russian).
Castaño, F. (1969). *Spectrochim. Acta Part A*, **25**, 401-405.
Devarajan, V. & Glazer, A. M. (1986). *Acta Cryst.* A**42**, 560-569.
Glazer, A. M. & Stadnicka, K. (1986). *J. Appl. Cryst.* **19**, 108-122.
Glazer, A. M., Stadnicka, K. & Singh, S. (1981). *J. Phys. C*, **14**, 5011-5029.
Grinter, R., Harding, M. J. & Mason, S. F. (1970). *J. Chem. Soc. A*, pp. 667-671.
Habrylo, S. & Koralewski, M. (1981). *Acta Phys. Pol. A*, **60**, 147-150.
Ingersoll, L. R., Rudnick, P., Slack, F. G. & Underwood, N. (1940). *Phys. Rev.* **57**, 1145-1153.
International Tables for X-ray Crystallography (1974). Vol. IV. Birmingham: Kynoch Press. (Present distributor D. Reidel, Dordrecht.)
Johnson, C. K. (1965). *ORTEP.* Report ORNL-3794. Oak Ridge National Laboratory, Tennessee.
Kato, T. (1972). *J. Phys. Soc. Jpn*, **32**, 192-201.
Kato, T., Ban, T. & Tsujikawa, I. (1972). *J. Phys. Soc. Jpn*, **32**, 152-157.
Kizel, V. A., Krasilov, Yu. I. & Burkov, V. I. (1974). *Usp. Fiz. Nauk.* **114**, 295-349 (in Russian).
Meredith, P. L. & Palmer, R. A. (1969). *Chem. Commun.* pp. 1337-1339.
Moscowitz, A. (1960). In *Optical Rotatory Dispersion*, by C. Djerassi. New York: McGraw-Hill.
O'Connor, B. H. & Dale, D. H. (1966). *Acta Cryst.* **21**, 705-709.
Perekalina, Z. B., Kaldybaev, K. A. & Konstantinova, A. F. (1979). *Kristallografiya*, **21**, 847-850 (in Russian).
Sheldrick, G. M. (1976). *SHELX76*. Program for crystal structure determination. Univ. of Cambridge, England.
Slack, F. G., Lageman, R. T. & Underwood, N. (1938). *Phys. Rev.* **54**, 358-360.
Strickland, R. & Richardson, F. S. (1972). *J. Chem. Phys.* **57**, 589-604.
Underwood, N., Slack, F. G. & Nelson, E. B. (1938). *Phys. Rev.* **54**, 355-357.
Winchell, A. N. & Winchell, H. (1964). *The Microscopical Characters of Artificial Inorganic Solid Substances: Optical Properties of Artificial Minerals.* New York: Academic Press.